Synthesis, molecular Docking, and anti-breast cancer study of 1-H-indol-3-Carbohydrazide and their derivatives

Article *in* Results in Chemistry · September 2024

DOI: 10.1016/j.rechem.2024.101762

5 authors, including:

Tahseen Alsalim
University of Basrah
29 PUBLICATIONS **268** CITATIONS
SEE PROFILE

Heider A. Abdulhussein
University of Kufa
29 PUBLICATIONS **398** CITATIONS
SEE PROFILE

Ahmed A. Majed
University of Basrah
23 PUBLICATIONS **102** CITATIONS
SEE PROFILE

Sabah Abbas
University of Kufa
26 PUBLICATIONS **43** CITATIONS
SEE PROFILE

Results in Chemistry 11 (2024) 101762

Contents lists available at ScienceDirect

Results in Chemistry

journal homepage: www.sciencedirect.com/journal/results-in-chemistry

Synthesis, molecular docking, and anti-breast cancer study of 1-H-indol-3-Carbohydrazide and their derivatives

Zainab H. Mahdi [a], Tahseen A. Alsalim [a,*], Heider A. Abdulhussein [b,c,*], Ahmed A. Majed [a], Sabah Abbas [d]

[a] Department of Chemistry, College of Education for Pure Sciences, University of Basrah, Basrah 61001, Iraq
[b] Department of Chemistry, Faculty of Science, University of Kufa, Najaf, Iraq
[c] College of Engineering, University of Warith Al-Anbiyaa, Kerbala, Iraq
[d] Department of Chemistry, Faculty of Education of Girls, University of Kufa, Najaf, Iraq

ARTICLE INFO

Keywords:
Indole derivatives
Triazol
Anticancer
MCF-7
CDK4
Molecular docking
Pharmacokinetic properties

ABSTRACT

A prominent heterocyclic system found in medications and natural goods is indoles. Due to the significance of this important ring system, a fresh batch of unique indole derivatives was created using indole carbohydrazide. The triazole moiety of indole derivative (3) is produced by reacting carbohydrazide with carbon disulfide in alkaline conditions, followed by hydrazine treatment. In addition to synthesizing additional derivatives, indole-bearing triazole (3) was condensed with aromatic aldehydes to create the indole derivatives (4a–c). Mass spectra, ^{1}HNMR, ^{13}CNMR, and infrared spectroscopy were used to diagnose all produced derivatives. An MTT assay was employed to test the derivatives against MCF-7 cells. The findings demonstrated the inhibitory action of compounds 5a and 5b, with IC50 values of 42.6 ± 0.33 μM and 27.3 ± 0.28, respectively. Affinity energy and the interaction between the investigated chemicals and receptor (CDK4 ID: 2w96) were ascertained by studying molecular docking. The chemical structure-physicochemical-pharmacokinetic relationship provides useful insight for medicinal chemists to design indole-triazole derivatives with acceptable drug-like and pharmacokinetic properties.

Introduction

The illness known as breast cancer is caused by aberrant breast cells that proliferate and develop into tumors [1]. Tumors can become deadly if they spread throughout the body and are not treated. Every nation experiences breast cancer [2]. In 2023, one in eight women (13 %) had a breast cancer diagnosis at some point in their lives [3]. These figures are somewhat higher than projections from 2022, which showed that there would be 51,400 new instances of ductal carcinoma in situ (DCIS) and 287,850 new cases of invasive breast cancer among women [4]. In 2020, breast cancer claimed 685 000 lives worldwide [5]. Worldwide, women without any particular risk factors other than age and sex account for around half of all cases of breast cancer [6]. From the 1930 s through the 1970 s, when surgery alone was the main form of therapy, there was minimal improvement in the death rate from breast cancer (radical mastectomy). Survival rates started to rise in the 1990 s when nations implemented early detection systems for breast cancer that were connected to all-encompassing treatment plans that included efficient pharmaceuticals [7].

Numerous heterocyclic compounds have been identified as possible anticancer agents in the last few decades [8,9]. Heterocyclic moieties provide the basis for around 60 % of the drugs used to treat cancer [10]. The required dose of anticancer medications is sufficient to eradicate cancer cells, but they also often damage healthy tissue and have several negative side effects, which limits the effectiveness of their treatment [11,12]. As a result, researchers are creating and investigating novel chemicals to find anticancer medications that will treat a variety of malignancies without having the negative side effects associated with traditional antineoplastic medications.

Indoles, a broad class of heterocyclic molecules abundant in nature that are essential to many bioactive natural and synthetic chemicals, have garnered a great deal of interest in recent years [13]. Numerous of these, including indapamide, pindolol, and indomethacin, have received drug approval [14]. A significant anticancer drug, indole-3-carbinol, likewise possesses the indole structure [15]. Bicyclic N-heterocycles like indole have The indole moiety containing benzene ring fused with 4

* Corresponding authors.
E-mail addresses: tahseen.alsalim@uobasrah.edu.iq (T.A. Alsalim), haydera.abdulhussein@uokufa.edu.iq (H.A. Abdulhussein).

https://doi.org/10.1016/j.rechem.2024.101762
Received 1 March 2024; Accepted 28 August 2024
Available online 6 September 2024

and 5 positions of pyrrole ring are widely spread in nature. Indole and its derivatives are well known to possess a broad spectrum of biological properties such as anticancer, antiviral, anti-fungal, anticonvulsant, ant tubercular, antimalarial, as well as their many biological effects [16–24]. Moreover, this ring has attracted a lot of attention as a favored pharmacophore for the creation of brand-new, extremely potent inhibitors [25]. The indole-3-carbohydrazide derivatives are a helpful family of synthetic chemicals that are utilized as a reagent to create novel molecules [26].

Indole derivatives were investigated for their potential anticancer properties. Several indole thiosemicarbazone derivatives were prepared and tested against the breast cancer cell line MCF-7. Strong action was shown by these compounds in destroying cancer cells and stopping their development [27]. 1, 2, 3–triazole tethered indole compounds were synthesized by D. Veeranna *et al.* Using the MTT test, those substances were examined for their potential to inhibit the growth of two human cancer cell lines, MCF-7 and HepG-2. A few of these substances demonstrated stronger effects on the MCF-7 and HepG-2 cell lines [28]. We have proposed the current work motivated by the known importance of Indoles in pharmacology. Indole-based compounds are found in a wide range of medications and natural stuff due to their various pharmacological activities. With them showing up in many of treatments, it is clear they could be the key to making new drugs. But, even with all that potential, research and health industry are always looking for ways to make them even better – more powerful, safer, and so on. This work aims to address this need by synthesizing a fresh batch of unique indole derivatives. Our method lets us whip up a whole range of them to test out. We're tackling the challenge of finding new indole versions that could fight breast cancer head-on, using a mix of lab work, tests, and computer models.

The present work highlights groundbreaking discoveries from the outset, focusing on the synthesis of a pioneering class of indole derivatives (1,3, 4a–4c, and 6a–6b). Furthermore, it delves into the investigation of these synthetic derivatives' cytotoxic potential against MCF-7 breast cancer cells, unveiling compelling results. Such findings hold immense promise as they suggest the potential of these compounds in halting cancer progression, showcasing comparable or superior efficacy to established cancer drugs such as Anastrozole, Lenvatinib, Vemurafenib, and Osimertinib. The efficient absorption of the obtained compounds and ability to traverse the blood–brain barrier, as indicated by the BOILED-Egg model study, further underpin their potential as promising treatments for breast cancer, heralding a new era of safer and more effective therapies compared to current standards.

Instrumentation and methods

Instrument

The chemical materials and solvents purchased from Merck, Sigma, and Fischer. Internal standard $Si(CH_3)_4$ (TMS) and solvent DMSO-d_6 were employed. Shimadzu FTIR (affinity-1) was used to record the IR spectra within the range 4000–400 cm^{-1}. EI mass spectra were measured on Agilent 7945 mass spectrometer.The ^1H and ^{13}CNMR spectra were examined using a Brucker 400 spectrometer. The coupling constants were measured in Hz and the chemical shift (δ) in ppm.

Procedures of synthesis

Synthesis indole-3-carbhydrazide (1)

16 ml of hydrazine hydrate was added to the reaction vessel containing 14.86 mmol, or 6.0 g, of indol-3-methyl carboxylate dissolved in 40 ml of ethanol. The mixture was heated for six hours. After the reaction cools to room temperature, the solid product is separated and refined by using ethanol to facilitate recrystallization.

Yellow crystal, ethanol was used for recrystallisation, yield (5.4 g, 90 %), m.p: 234–235 °C, ^{1}HNMR (400 MHz, DMSO-d_6) δ 11.55 (s,1H, NH), 9.18 (s, 1H, indole-NH), 8.16 (d, 1H, *J*=8, Ar-H), 7.99 (s, 1H, Ar-CH-N), 8.16 (d, 1H, *J*=8, Ar-H), 8.16 (m, 2H, Ar-H), 4.43(s, 2H, NH_2). ^{13}CNMR (100 MHz, DMSO-d_6) δ, 165.6, 136.4, 127.5, 126.6, 121.4, 120.7, 112.2, 109.4. IR (υ, cm^{-1}): 3300 (NH), 3205–3180 (NH_2), 3047 (C-H sp^2) 1618 (C=O), 1575 (C=C), 1539 (C-O). MS: EI (70 eV, *m/z*), 175.1 [M^+], 144.0 (base peak), 166, 89, 63.

Synthesis 4-amino-5-(1H-indol-3-yl)-4H-1,2,4-triazole-3-thiol (3)

(**a**) A solution of 0.2 g potassium hydroxide in 20 ml of distilled water and 1 ml of CS2 was added to 20 ml ethanol in a 100 ml reaction flask along with indole-3-carbohydrazide (1) (0.92 g, 4 mmol). Thin-layer chromatography (TLC) was used to monitor the reaction mixture, which was heated using reflux and a solvent system consisting of ethanol and chloroform in a 1:9 vol ratio. The reaction was cooled after six hours, and the byproducts were filtered and then recrystallized the product compound 2 from ethanol.

(**b**) (1.4 g, 5 mmol) from the product (part a compound 2) was taken and dissolved in 40 ml ethanol in a 100 ml reaction vessel. It was then heated under reflux while 5 ml of hydrazine hydrate was added and stirred. TLC was used to monitor the reaction (1:9 v/v, EtOH: $CHCl_3$). The reaction was cooled after six hours, at which point the solid product was filtered out and recrystallized from ethanol. [29].

Orange powder, recrystallized from ethanol, yield(0.73 g, 66 %), m.p: 199–200 °C, IR (υ, $cm^{-}1$): 3302 (NH),3248–3215 (NH_2), 3068 (C-H sp^2), 1637 (C=N), 1616 (C=C),1510, 1447 (C-O), 1382 (C-N). ^{1}HNMR (400 MHz, DMSO-d_6) δ 9.20 (s, 1H, indole-NH), 8.20 (d, 1H, Ar-H), 8.04 (s, 1H, Ar-H), 7.57 (d, 1H, *J*=4, Ar-H), 7.25(m, 2H, *J*=4, Ar-H), 5.9(s, 2H, NH_2). ^{13}CNMR (100 MHz, DMSO-d_6) δ, 172.6, 145.1, 135.4, 127.7, 125.4, 122.4, 119.8, 111.8, 105.9. MS: EI (70 eV, *m/z*), 231.2 [M^+], 217.1 (base peak), 157.1, 142.1, 130.1, 115.1, 103.1, 89.1, 76, 63.

General procedure synthesis indol-triazol derivatives (4a-c)

Compound (3) (1.18 g, 4 mmol) dissolved in 40 ml ethanol in 100 ml reaction vessel, aromatic aldehyde (4-dimethoxy benzaldehyde, 4-anthraldehyde, piperonal) (4 mmol) was added, and a few drops of glacial acetic acid as a catalyst was added, the reaction mixture was heated by reflux and monitored by TLC (EtOH: $CHCl_3$, 2:8 v/v). After 7 h, the reaction was cooled, and the products were collected by filtration and purified by recrystallization using ethanol. [30].

(E)-5-(1H-indol-3-yl)-4-((4-methoxybenzylidene)amino)-4H-1,2,4-triazole-3-thiol (4a). Orange powder, yield (1.06 g, 76 %), m.p: 238–240 °C, IR(υ,cm^{-1}) 3437 (NH), 3030 (CH sp^2), 2916 (CH sp^3), 1647 (C=N), 1600 (C=C), 1543, 1525 (C-O), 1348 (NH). ^{1}HNMR (400 MHz, DMSO-d_6) δ, 9.69 (s, 1H, indole-NH), 8.78 (s, 1H, CH=N), 8.20 (s, 1H, Ar-H), 7.85(d, 2H, *J*=8, Ar-H), 7.71(d, 1H, *J*=8, Ar-H), 7.28(d, 2H, *J*=8, Ar-H), 6.85(m, 2H, Ar-H), 3.84 (s, 3H, OCH_3). ^{13}CNMR (100 MHz, DMSO-d_6) δ, 168.5, 162.1, 160.9, 152.4, 150, 145.7 138.4, 137.1, 133.9, 130.4, 127, 125.5, 121.8, 117, 114.8, 112.8, 111, 57.4, 55.8. MS: EI (70 eV, *m/z*), 394.3 [M^+], 294.2, 266.3, 251.3, 174.2, 147.1 69.1 (base peak).

(E)-5-(1H-indol-3-yl)-4-((4-methoxybenzylidene)amino)-4H-1,2,4-triazole-3-thiol (4b). Orange powder, yield (1.34 g, 84 %), m.p: 254–256 °C, ^{1}HNMR (400 MHz, DMSO-d_6) δ 9.48 (s, 1H, indol-NH), 8.89 (s, 1H, CH=N), 7.09 – 8.27 (Ar-H), IR(υ, cm^{-1}) 3431 (NH), 3039 (CH sp^2), 1670 (C=N), 1608 (C=C), 1328 (C-N), 1159 (C=S), MS: EI (70 eV, *m/z*) 419.4 [M^+], 229.1, 204.1 (base peak), 177.1, 151.0, 88.0, 63.0.

(E)-4-((benzo[d][1,3]dioxol-5-ylmethylene)amino)-5-(1H-indol-3-yl)-4H-1,2,4-triazole-3-thiol (4c).

Orange powder, yield (1.1 g, 76 %), m.p: 211–213 °C, ^{1}HNMR (400 MHz, DMSO-d_6) δ 9.4 (s,1H, indol-NH), 8.81 (s, 1H,CH=N), 7.83 (d, IH, Ar-H), 7.59(m, 3H, Ar-H), 7.55(m, 1H, Ar-H), 7.45(m, 1H, Ar-H), 7.42 (d, 1H, Ar-H), 7.32(t, 1H, Ar-H), 7.07(m, 1H, Ar-H), 6.14(s, 2H, O-CH_2-O), IR(υ, cm^{-1}) 3431 (NH), 3020 (CH sp^2), 2019 (CH sp^3)1651 (C=N),

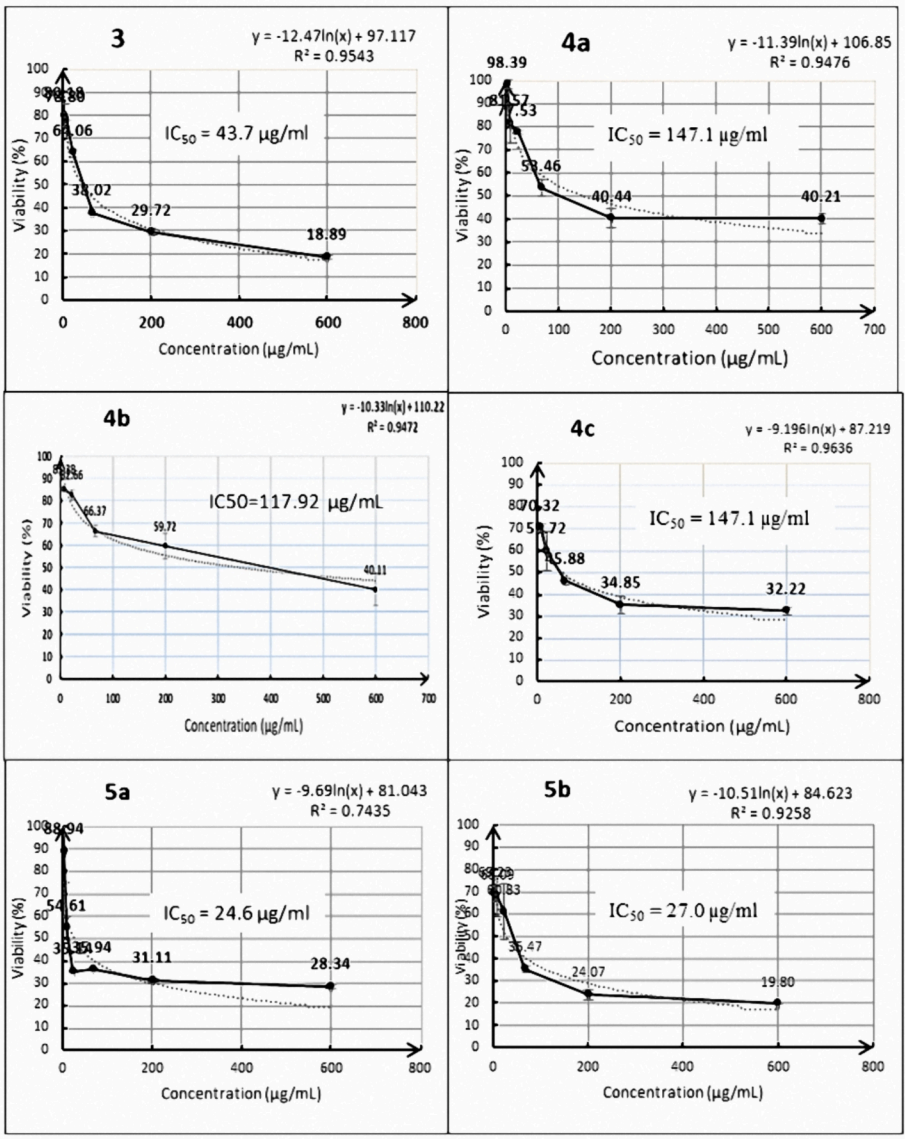

Fig. 1. IC50 estimation of studied compounds using MTT assay.

1620 (C=N), 1620 (C=C), 1261 (C-N), 1031 (C=S).

Synthesis procedure of indol-benzylidene (5a, 5b)

Using glacial acetic acid as a catalytic agent, ethanolic solutions of the amine and aldehyde were combined at room temperature in a 1:1 M ratio. For five hours, the resultant mixture was refluxed. After the solution was allowed to stand for a few hours at 25 °C, the crystalline product was extracted. After filtering out the precipitate. The pure chemical was extracted from ethanol by recrystallization.

(E)-N'-(4-methoxybenzylidene)-1H-indole-3-carbohydrazide (5a). White crystal, recrystallized from ethanol, yield (1.6 g, 85 %), m.p: 249–250 °C, IR (υ, cm $^{-1}$)3253 (NH), 3053(CH sp^2), 1622(CH=N), 1697 (C=O), 1581(C=C), 1269(C-F_3) 1323 (C-N), ^{1}HNMR (400 MHz, DMSO-d_6) δ, 11.74 (s, 1H, NH-C=O), 11.28 (s, 1H, indol-NH), 8.24 (s, 1H, CH=N), 8.22(s, 1H, Ar-H), 7.67 (d, 2H, *J*=8, Ar-H), 7.51(d, 1H, Ar-H), 7.22(d, 1H, *J*=8, Ar-H), 7.16(m, 2H, Ar-H), 7.02(d, 2H, Ar-H), 3.82 (s, 3H, OCH_3), ^{13}CNMR (100 MHz, DMSO-d_6) δ 167.51, 161.21, 148.45, 150.52, 139.58, 135.89, 130.65, 128.79, 125.63, 122.35, 118.66, 112.32, 109.08, 106.46, 102.21. MS: EI (70 eV, *m/z*) 331.1 [M$^+$], 159.0, 144.0 (base peak), 89.0,63.0.

(E)-N'-(4-(trifluoromethyl)benzylidene)-1H-indole-3-carbohydrazide (5b). White crystal, recrystallized from ethanol, yield (0.85 g, 80 %), m.p: 240–241 °C, IR(υ, cm^{-1}) 3338 (NH), 3016 (CH sp^2), 1637 (C=O), 1573 (C=C), 1606 (C=N), 1180 (C-O), ^{1}HNMR (400 MHz, DMSO-d_6) δ 11.81 (s, 1H, NH-C=O), 11.62 (s, 1H, indol-NH), 8.85 (s, 1H, CH=N), 8.40—7.15 (9H, Ar-H).^{13}CNMR (100 MHz, DMSO-d_6) δ 150.44, 167.0,160.91, 157.59, 55.76, 144.46, 138.85, 135.46, 128.75, 127.86, 122.65, 121.15, 114.42, 112.40, 108.48, 105.57, 102.4. MS: EI (70 eV, *m/z*) 239.1 [M$^+$], 160.1, 144.0(base peak), 116.0.

MTT cell viability assay

The MTT [3-(4, 5-dimethylthiazol-2-yl)-2, 5-diphenyltetrazolium Bromide] (Sigma-Aldrich) test was used to measure the proliferation and vitality of the cells. In a nutshell, trypsin was used to break down the cells, after which they were extracted, adjusted to a density of 1.4 × 104 cells/well, and seeded onto 96-well plates containing 200 µl of fresh media each well for 48 h. The cells were exposed to 600–7.4 µg/ml of the compounds for 48 h at 37 °C in 5 % CO2 after they had established a monolayer. After 48 h of treatment, the supernatant was discarded, and 200 ÂµÌ per well of MTT solution (0.5 mg/ml in phosphate-buffered saline; PBS) was added. The plate was then incubated at 37 °C for an

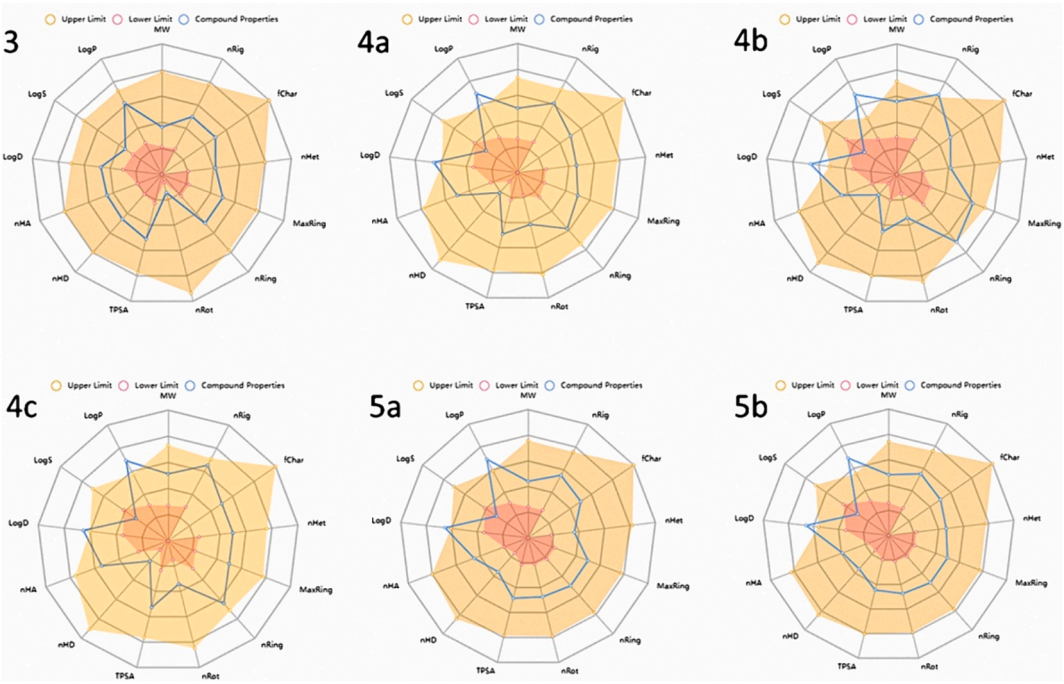

Fig. 2. Bioavailability Radar related to physicochemical properties of molecules (criteria: lipophilicity: 1.45 < XLOGP3 < 5.93, size: 231 < MW<419 g/mol, polarity: 66.48 < TPSA<107.89 Å^2, flexibility: 2 < rotatable bonds < 5).

extra four hours, all the while keeping the monolayer culture intact in the original plate. MTT solution: 100 μl of dimethyl sulfoxide was added to each well after the cell supernatant was collected. On a shaker, the cells were incubated at 37 °C until the crystals were entirely dissolved. Using an ELISA reader (Model wave xs2, BioTek, USA), absorbance at 570 nm was used to quantify the vitality of the cells. Using the appropriate dose–response curves, the concentration of the chemicals that caused 50 % of cell death (IC50) was found. the (IC50), were calculated by the following equation [31,32].

$$Viability\% = \frac{meanofODsample}{meanofODcontrole} x10$$

Results and discussions

Anticancer activity

In the past few decades, particularly during the 1950 s, the development of numerous heterocyclic compounds and indole derivatives as anticancer agents has been widely recognized [33–35]. Indole derivatives have gained significant importance as medicinal drugs, with many traditional medications incorporating indole as an essential component. These compounds are utilized in cancer treatment either by directly targeting and poisoning cancer cells or by inhibiting their growth. For instance, Anastrozole, a nonsteroidal drug, is commonly prescribed for the treatment of breast cancer in women [36]. It functions by reducing the production of estrogen in the body, thus slowing down or reversing the growth of estrogen-dependent breast cancers. Similarly, Lenvatinib is employed in the treatment of specific types of thyroid cancer and hepatocellular carcinoma (HCC) that are not amenable to surgical intervention [37]. Its mechanism of action involves blocking the activity of abnormal proteins that stimulate the proliferation of cancer cells, thereby impeding their spread. Furthermore, Vemurafenib serves as a targeted therapy for melanoma skin cancer that cannot be surgically removed [38]. By inhibiting cancer cell growth, it acts as a "cancer growth blocker." Similarly, Osimertinib, another cancer growth blocker, targets proteins within cancer cells to impede their growth, particularly in advanced cancers [39]. Post-surgery, Osimertinib may aid in preventing cancer recurrence. Despite their effectiveness in killing cancer cells, conventional anticancer drugs often come with significant drawbacks. They frequently cause harm to healthy tissues and are associated with various adverse effects, including alterations in heart rate, nervousness, chest discomfort, blurred vision, headaches, and bone pain. Consequently, there is a pressing need for the development of new compounds with improved efficacy and safety profiles. Scientists are actively engaged in the exploration and development of novel anticancer drugs that possess the potential to treat a wide range of cancers without the unfavorable side effects commonly associated with conventional chemotherapeutic agents. These efforts aim to revolutionize cancer treatment by providing safer and more effective therapeutic options for patients.

After lung cancer, breast cancer (BC) is the second most prevalent cause of cancer-related deaths among women. Current medicines, such as hormone therapy, surgery, radiation, and chemotherapy, often become ineffective due to significant side effects and multidrug resistance. Additionally, the medications currently used to treat BC have several drawbacks, including poor pharmacodynamic qualities, lack of selectivity, and low oral bioavailability. Despite significant progress in cancer research and therapy, BC remains a challenging medical issue and a top priority for biomedical research. The development of safer and more potent anti-breast cancer drugs is therefore urgently needed [40–43].

The objective of the current investigation is to ascertain the anticancer activity of a class of indole and triazole against the MCF-7 breast cancer cell line. We aimed to explore the anticancer potential of novel indole derivatives against the MCF-7 cell line. MTT tests were employed to assess the cytotoxicity of all indole derivatives.

Highly effective chemicals were identified using a six-dose (2.5 μM, 7.5 μM, 20 μM, 75 μM, 200 μM, and 600 μM) screening panel in the MCF-7 breast cancer cell line. Consequently, the majority of the compounds exhibited robust activity in the MCF-7 main anticancer activity test.

In this study, we investigated the effects of six novel indole derivatives on MCF-7 breast cancer cells, observing anticancer activity within the range of (24.6–145.8) mM (Fig. 1). Notably, compound 5a demonstrated the most potent activity (IC50 24.6 μg), followed by 5b

Table 1
Shows the computer-generated admet profile prediction for indole derivatives.

Indole derivatives Parameter	3	4a	4b	4c	5a	5b
Absorption						
Human intestinal absorption (HIA)	0.015	0.12	0.121	0.007	0.007	0.005
Caco-2 permeability (log Papp in 10^{-6} cm/s)	0.145	0.914	1.364	0.997	1.149	1.403
Intestinal absorption (Human) (%)	90.903	91.868	91.326	90.379	93.16	94.177
Water solubility(log mol/L)	−2.785	−3.868	−4.689	−2.739	−3.906	−4.42
Skin Permeability (log kp)	−2.794	−2.379	−2.735	−3.673	−2.826	−2.791
Distribution						
VDss (human) (log L/kg)	−0.166	−0.169	−0.673	−0.151	−0.05	−0.019
Fraction unbound (human) Fu	0.257	0.059	0.256	0.09	0	0
BBB permeability(log BB)	−0.802	−0.299	0.529	−0.8	0.091	0.181
CNS permeability (log ps)	−2.344	−2.165	−1.536	−2.301	−2.13	−1.787
Plasma protein binding (PPB)	98.31 %	96.59 %	97.31 %	97.184 %	98.639 %	99.087 %
Medicinal chemistry						
QED	0.438	0.437	0.213	0.432	0.573	0.554
SA score	2.660	2.501	2.634	2.699	1.913	2.096
Fsp^3	0.000	0.056	0.000	0.56	0.059	0.059
MCE-18	15.000	20.000	29.000	50.526	15.000	18.000
NP score	−1.602	−1.476	−1.094	−1.263	−1.312	−1.576
Lipinski Rule	Accepted	Accepted	Accepted	Accepted	Accepted	Accepted
Pfizer Rule	Accepted	Rejected	Rejected	Accepted	Rejected	Rejected
GSK Rule	Accepted	Rejected	Rejected	Rejected	Rejected	Rejected
Golden Triangle	Accepted	Accepted	Accepted	Accepted	Accepted	Accepted
		Metabolism				
CYP1A2 inhibitor	+++	+++	+++	+++	+++	+++
CYP1A2 substrate	−	+	−-	−-	++	−
CYP2C19 inhibitor	++	+++	+++	+++	++	++
CYP2C19 substrate	− − −	− −	− − −	− − −	− −	− − −
CYP2C9 inhibitor	++	++	+++	++	++	++
CYP2C9 substrate	++	+++	++	++	+++	++
CYP2D6 inhibitor	−-	+	++	+++	−	− −
CYP2D6 substrate	++	++	++	+	++	++
CYP3A4 inhibitor	+	++	+++	+++	++	+
CYP3A4 substrate	− −	+	− −	− −	− −	−
Toxicity						
AMES toxicity	Yes	Yes	Yes	No	Yes	Yes
Max. tolerated dose (human) (log mg/kg/day)	0.053	0.523	0.524	0.551	0.272	0.241
hERG I inhibitor	No	No	No	No	No	No
hERG II inhibitor	No	yes	No	Yes	Yes	Yes
Oral Rat Acute Toxicity (LD50) (mol/kg)	3.273	3.302	2.464	3.123	2.088	2.258
Oral Rat Chronic Toxicity (LOAEL) (log mg/kg_bw/day)	1.197	1.298	−0.617	0.69	1.841	1.725
Hepatotoxicity	No	Yes	Yes	Yes	Yes	Yes
Skin Sensitisation	No	No	No	No	No	No
T.Pyriformis toxicity (log ug/L)	0.351	0.3	0.285	0.291	0.636	0.707
Minnow toxicity (log mM)	0.565	0.95	−5.05	−1.587	−0.61	−0.216

derivative (IC50 27.0 μg), and then 3 (IC50 43.7 μM). Conversely, compounds 4a, 4b, and 4c displayed lower activity, with IC50 values of 147.9, 117.9, and 145.8 μM, respectively.

These results suggest a potential role of substituted groups in the activity of compounds 5a and 5b. The variance in activity could also be attributed to structural factors, implying that the indole derivatives may form additional interactions with specific biological targets. The heightened activity of 5a and 5b further indicates that physicochemical parameters (such as molecule flexibility and conformation in the protein active site), as well as the carbonyl, methoxy, and trifluoromethane groups, may contribute to the anti-cancer activity[44].

The activity of compound 3 can be attributed to the presence of the free amino group and the triazole ring, which enhances its ability to bind to the active site of the target protein. On the other hand, compounds 4a-c exhibit lower cytotoxic activity compared to other derivatives. This difference in activity could be attributed to the structural rigidity of these molecules, stemming from the presence of aromatic rings linked to the triazole ring. These aromatic rings reduce flexibility due to the low number of rotatable bonds, implying a decreased level of flexibility [32]. Thus, the molecule is unstable within the active site, which diminishes its ability to occupy and bind with the residues of the protein in the active site and subsequently adopt the appropriate conformation within the active site of the protein, thereby disrupting the cancer cell and inducing its demise.

Pharmacokinetic and drug-likeness properties (ADMET)

Understanding the pharmacokinetic and drug-like characteristics of newly discovered compounds for specific targets is essential for predicting the absorption, distribution, metabolism, and excretion of potential novel therapeutic leads [45]. This study utilized the website http://www.swissadme to analyze the physicochemical characteristics of potent hits in silico, employing ADME analysis (absorption, distribution, metabolism, and excretion). These characteristics encompassed water solubility, lipophilicity, and pharmacokinetics. The following formula was applied to ascertain the % ABS (percentage of potent hits absorbed) from the gut: ABS% ¼ 109 = 0.345 XTPSA.

The pharmacokinetic characteristics of the investigated drugs were predicted using the SwissADME program (Fig. 2). With molecular weights of less than 400 g/mol, 1–4 hydrogen bond donors, 2–5 acceptors, a log P value of less than 5, and a molar refractivity of less than 130, we found that every molecule adhered to Lipinski's rule of five[46]. According to Shivanika [47], every molecule has a Topological Polar Surface Area (TPSA) of less than 110 $Å^2$, indicating that they may be able

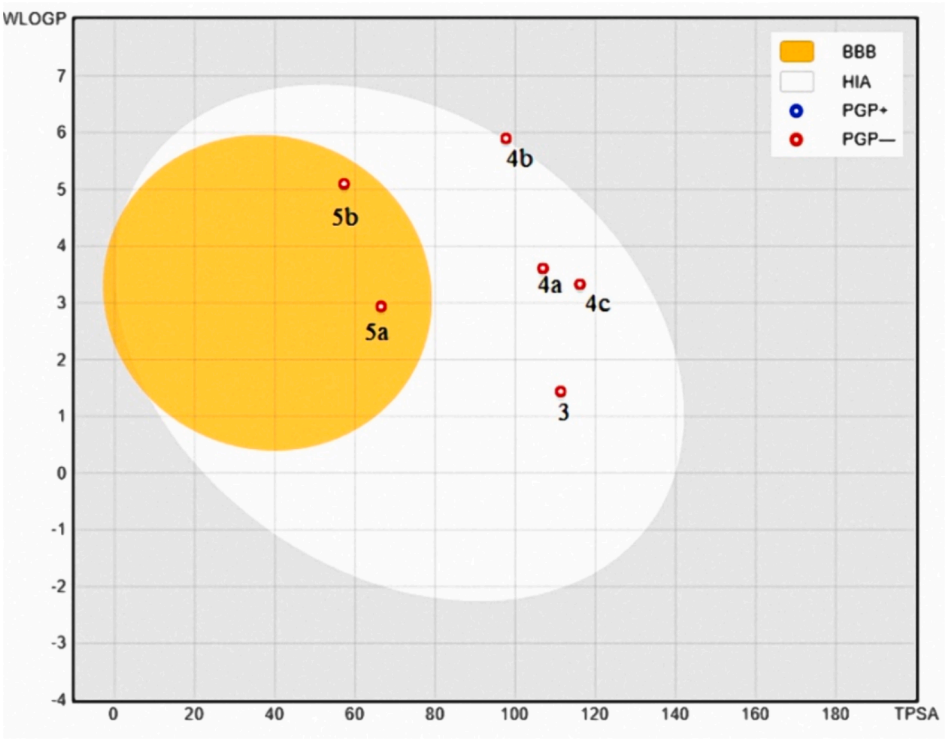

Fig. 3. BOILED-Egg model of studied indole derivatives.

to pass through biological membranes[48].

All chemicals also exhibit good solubility and gastric absorption. The presence of numerous rotatable bonds (1–5) suggests a high degree of flexibility. The toxicity of the compounds under study was assessed using the pkCSM software program (https://structure.bioc.cam.ac.uk/pkcsm) (Table 1). We observed that derivatives 5a and 5b demonstrated superior toxicity profiles and were found to be non-carcinogenic and non-hepatotoxic. Interestingly, these compounds displayed the highest penetration rates among all compounds, with log P values ranging from 4.071 to 4.697. This suggests that these compounds can efficiently traverse biological membranes [49,50]. This is compatible with its IC50 value and enhances its binding capacity with MCF-7 proteins.

Relationship studies of structure activity

Based on our in vitro findings, it appears that compounds 5a and 5b exert a stronger effect on MCF-7 cells compared to other derivatives. Compound 5a features a carbonyl of an amide group bound to an indole ring, while compound 5b exhibits an azomethine group connected to an aromatic ring, along with trifluoromethane and methoxy groups linked to the aromatic ring. Incorporating heteroatoms and functional groups enhances the binding potential of these compounds with MCF-7 cells. Specifically, these groups are likely to form strong interactions with the amino acid residues of the target protein and are excellent candidates for hydrogen bonding [51]. The presence of diverse functional groups enhances the effectiveness of these compounds against breast cancer cells, thereby warranting further investigation.

Boiled-egg for estimating brain penetration and GI absorption.

Blood-brain barrier (BBB) penetration and GI absorption are critical steps in the medication development process. The BOILED-Egg model provides datasets with precision, speed, and easily comprehensible graphical representations, aiding in the estimation of derivatives' polarity and lipophilicity [52]. This model facilitates the creation of new drugs. The white zone of the BOILED-Egg model indicates a high chance of passive GI tract absorption, while the yellow portion (yolk) represents a high probability of BBB penetration. Furthermore, the molecule's blue color indication suggests that P-glycoprotein is actively effluxing the molecule (PGP+), whereas the red color indicator suggests that Pgp is not a substrate (PGP−). According to the research, molecules 5a and 5b are expected to demonstrate significant GI absorption and BBB penetration. They are also predicted to be nonsubstrates of P-gp (PGP−). Fig. 3 depicts the BOILED-Egg model prediction of GI absorption and BBB permeability of the indole derivatives 5a and 5b that were ultimately examined.

Molecular docking study

Currently, molecular bioinformatics docking studies are highly valuable in the drug development industry as they reduce the cost and effort required to screen new compounds by focusing on potential targets [53]. Therefore, one of the most important methods to predict how a substrate will interact with its receptor is through molecular docking simulations. By determining the binding mode of indole derivatives into the CDK4 active site through molecular docking modeling, it was possible to ascertain whether the investigated compounds block CDK4 proteins and, consequently, alter the cellular migration of MCF-7 [54]. Using ADT software, the examined compounds were accurately docked into CDK4′s active pocket. The findings of the docking study demonstrated an excellent fit into the binding site of the CDK4 protein, with affinity energies ranging from −9.25 kJ/mol to −7.25 kJ/mol. Additionally, Table 2 and Figs. 4 and 5 depict the binding interactions between the amino acid residues and ligands. According to the docking results, compounds 5a and 5b exhibited the best affinity energies (−9.25 kJ/mol and −9.21 kJ/mol, respectively) among the other derivatives. This aligns with the findings of the breast cancer test, where they provided the lowest IC50 values. Compound 5a formed two hydrogen bonds, as a side-chain acceptor and backbone acceptor with amino acid residues (ARG 62B and ASN 134B) of the CDK4 protein. Additionally, several hydrophobic interactions with amino acid residues

Table 2
Affinity energy and amino acids residue of Indole derivatives with CDK4 protein.

Target protein	PDB ID	Compound	Binding interaction (Amino acid residue)	Interaction	Distance	RMSD	Affinity energy (Kcal/mol)	Estimated inhibition constant (Ki)
					(A°)	(A°)		
			GLU 56B	H-donor	2.77			
			VAL 137B	H-donor	3.01			
		3	LEU 59B	Pi-Alkyl	3.01	63.88	−8.41	3.69
			LEU 60B	Pi-Alkyl	3.1			(micromolar)
			ILE 136B	Pi-Sigma	3.87			
			ILE 136B	Pi-Alkyl	3.39			
			VAL 137B	H-doner	2.19			
CDK4	2 W96		ARG 160B	H-doner	2.99			
		4a	ALA 162B	H-doner	3.32	62.59	−8.8	351.66
			LEU 59B	Pi-Alkyl	3.34			(nanomolar)
			LEU 59B	Pi-Alkyl	3.11			
			LEU60B	Pi-Alkyl	3			
			ILE 136B	Pi-Sigma	3.86			
			VAL 137B	Pi-Sigma	3.21			
		4b	CYS 135B	H-donor	3.48		−9.5	
			LEU 59B	Pi-Alkyl	3.25			
			ILE 136B	Pi-Alkyl	3.73	61.68		108.6
			ILE 136B	Pi-Alkyl	3.9			(nanomolar)
			VAL 137B	Pi-Alkyl	3.38			
			VAL137B	Vander waals	3.39			
			ARG 139B	Pi-Alkyl	3.19			
			ALA 162B	Pi-Alkyl	3.48			
			TYR 191B	Vander waals	3.58			
		4c	CYS 135B	H-donor	3.17		−7.25	4.88
			ALA 162B	H-donor	3.93			(micromolar)
			LEU 59B	Pi-Alkyl	3.28	62.61		
			LEU 60B	Pi-Alkyl	3.13			
			ILE 136B	Pi-Sigma	3.66			
			ILE 136B	Pi-Sigma	3.78			
			VAL 137B	Pi-Sigma	3.52			
			ARG 62B	H-doner	2.9			
			ASN 134B	H-doner	2.96			
		5a	LEU 59B	Pi-Alkyl	3.36	60.809	−9.25	901.62
			ASN 134B	Pi-H	3.93			(nanomolar)
			ILE 136B	Pi-Alkyl	3.34			
			VAL 137B	Pi-Alkyl	3.65			
			GLU 56B	H-donor	3.57			
		5b	VAL 137B	H-donor	2.56			5.19
			ARG 163B	H-donor	3.6	61.45	−9.21	(micromolar)
			ARG 163B	Pi-Cation	5.84			
			LEU 59B	Pi-Sigma	3.45			
			ILE 136B	Pi-Alkyl	3.2			
			VAL 137B	Pi-Alkyl	3.25			

including LEU 59B, ASN 134B, ILE 136B, and VAL 137B were observed. Compound 5b formed three hydrogen bonds as a side-chain acceptor with amino acid residues (GLU 56B, VAL 137B, and ARG 163B), in addition to hydrophobic interactions with amino acid residues including ARG 163B, LEU 59B, ILE 136B, and VAL 137B. Fig. 6 displays the active site of MCF-7 with compounds 5a and 5b docked into the binding site.

Chemistry

The indole scaffold is renowned as a model for synthesizing compounds with anticancer properties. Indoline derivatives, in particular, hold significance as anti-breast cancer agents, sparking considerable interest in the synthesis of pharmacologically potent indole derivatives in recent years. Additionally, indole is present in numerous natural products, some of which are utilized as antitumor medications. For instance, Vinblastine and Vincristine, dimeric alkaloids isolated from the Madagascar periwinkle plant, are widely employed in antitumor therapy [55].

Indole derivatives exhibit potent anticancer activity against various types of cancers, including bone cancer and brain tumors [5657]. They have been shown to inhibit the proliferation of breast cancer cells and induce apoptosis in cancerous cells [58–60]. Previous studies have demonstrated the cytotoxic effects of indole derivatives on MCF7 tumor cells while sparing non-cancerous cells [61].

Given this evidence, there has been a concerted effort to synthesize new indole derivatives to further investigate their efficacy against breast cancer cells, which represent the leading cause of death in women. These endeavors aim to expand our understanding of this class of compounds and potentially develop novel therapeutic options for breast cancer treatment.

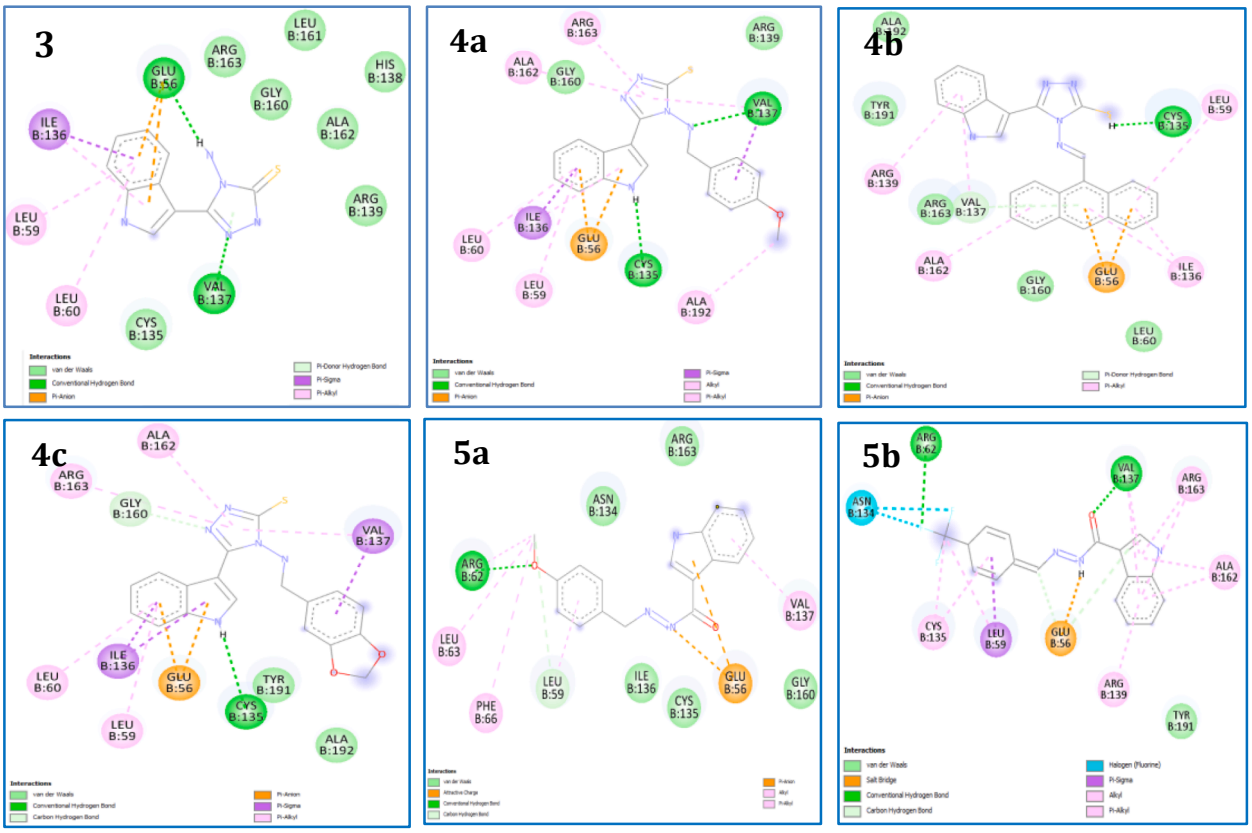

Fig. 4. Two dimensional indole derivatives interact with the active site of target protein CDK4.

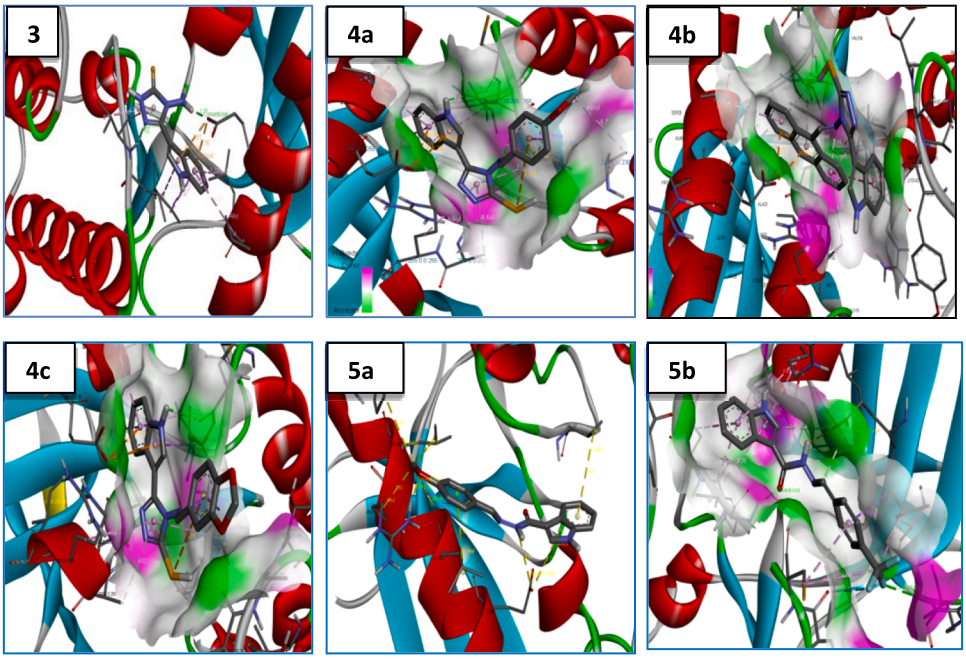

Fig. 5. Three dimensional indole derivatives interact with the active site of target protein CDK4.

As shown in Fig. 7, the pathway of the synthesis of indol derivatives are outlined. The synthesis of indole derivatives involves multiple steps. Initially, 3-indolecarbohydrazide (1) is synthesized from methyl indole-3-carboxylate by reacting it with hydrazine in ethanol as a solvent. Compound 1 serves as a starting material for synthesizing the indole derivatives. It is then treated with carbon disulfide in alkaline media to prepare potassium 2-(1H-indole-3-carbonyl)hydrazine-1-carbodithioate (2), followed by the addition of hydrazine hydrate and potassium hydroxide to compound 2 to obtain indole-3-triazole (3). The Schiff bases of indole triazole derivatives (4a-c) are prepared by condensing corresponding aromatic aldehydes with indole-3-triazole in a 1:1 M ratio, with a few drops of acetic acid as a catalyst under reflux. Other indole

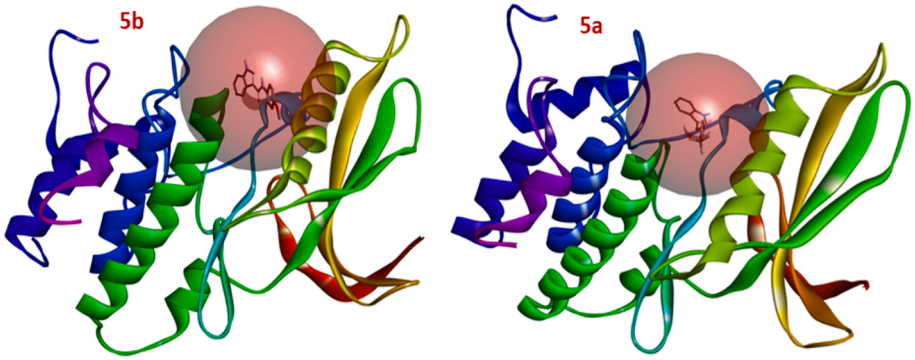

Fig. 6. Show the binding of ligands (5a and 5b) with the active site of MCF-7.

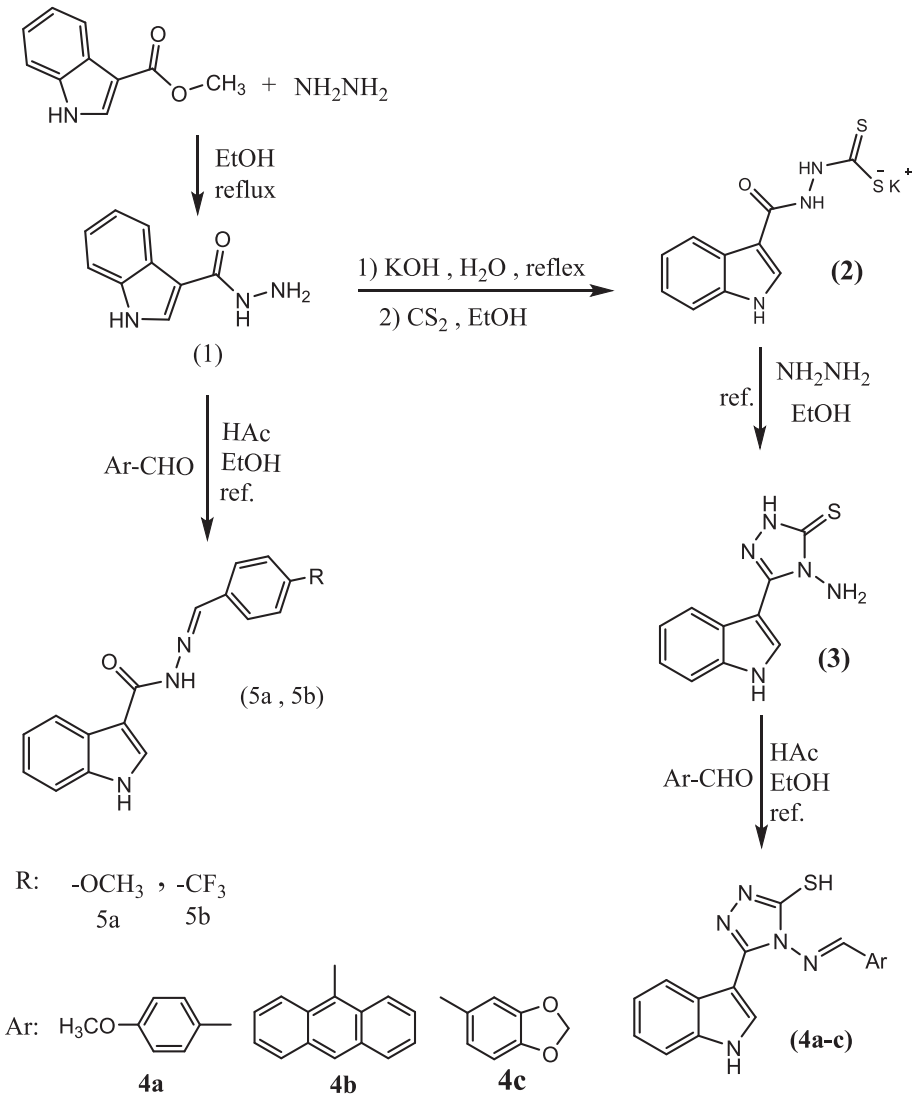

Fig. 7. Synthesis pathway of indole derivatives.

derivatives (5a and 5b) are prepared from the reaction of 3-indolecarbohydrazide (1) with the corresponding aldehyde to form Schiff bases of indole.

The synthesized indole derivatives are characterized using spectroscopic techniques such as infrared spectroscopy, electron impact mass spectroscopy, as well as proton carbon nuclear magnetic resonance. These techniques validate the suggested structures of the synthesized indole derivatives.

The bioactivity of the indole derivatives is evaluated for their anticancer activity against breast cancer (MCF-7), and molecular docking studies are conducted on a target protein (CDK4 ID: 2w96). Additionally, the pharmacokinetics and drug-like characteristics of the newly discovered compounds are studied.

Spectral characterization

The infrared spectra of the synthetic compounds exhibit bands corresponding to the expected functional groups. In the indolecarbohydrazide IR spectrum, two bands at 3300 and 3205 cm^{-1} are attributed to symmetric and asymmetric stretching of the amine group, while the strong band at 1618 cm^{-1} is attributed to the carbonyl stretching vibration of the amide, a behavior documented in the literature [62]. For indole-3-triazole (3), the IR spectrum displays two bands at 3302 cm^{-1} and 3248 cm^{-1}, attributed to the symmetric and asymmetric stretching vibrations of the amino group, along with a strong band at 1637 cm^{-1} attributed to the C=N bond of the triazole ring. The IR spectra of indole-3-triazole derivatives (4a-c) exhibit a strong band within the range of 1705–1770 cm^{-1}, attributed to the azomethine (CH=N) of the Schiff base formed from the condensation of the corresponding aldehyde with the amine of indole-3-triazole.

The IR spectra of indole derivatives (5a and 5b) display two strong bands at 1622 and 1637 cm^{-1}, and bands at 1602 and 1606 cm^{-1} for the carbonyl of the amide and the azomethine, respectively.

The ^{1}H NMR spectrum data of the synthesized compounds at room temperature in deuterated DMSO confirms the heterocyclic ring formation and the structure of compounds annotation. Indole carbohydrazide (1) exhibits two signals of carbohydrazide at 11.55 ppm and 4.34 ppm attributed to NH and NH_2 respectively, along with a singlet signal at 9.18 ppm attributed to indole NH, signals within the 7.11–8.18 ppm range attributed to aromatic protons,. The indol-3-triazole (3) displays a singlet signal at 9.20 ppm for the NH proton of indole, a singlet signal of NH_2 protons at 5.90 ppm, and signals within the range (7.20–8.20) ppm attributed to the aromatic protons. All protons in their predicted area are observed. The indole derivatives (4a-c) display a singlet signal within the range (8.89–8.78) ppm attributed to the azomethine proton, a singlet signal of NH proton of indole appears at (9.69–9.40) ppm, as well as signals of the aromatic protons within the range (7.83–7.07)ppm. The spectrum of compound 4a shows a singlet signal at 3.84 ppm belonging to the methoxy group while the spectrum for compound 4c has a singlet signal for O-CH_2-O at 6.14 ppm. A comparison of indol-3-triazole chemical shifts with derivatives (4a-c) indicates that the NH_2-protons signal in the spectrum of derivatives is absent. Also, we observed the absence of the NH_2 signal from the 5a and 5b spectra due to its reaction and the formation of the azomethine group compared to its presence in the indole carbohydrazide spectrum. Therefore spectra of indole derivatives (5a and 5b) show a singlet signal at 8.24 ppm and 8.85 ppm respectively attributed to the azomethine proton[30]. The ^{1}HNMR, ^{13}CNMR, as well as mass spectra (Figure S1-S26), truly confirm the suggested structure for synthesized newly indole derivatives.

Conclusion

A novel class of indole derivatives (1,3, 4a–4c, and 6a–6b) has been synthesized. Additionally, we investigated the synthetic derivatives' cytotoxic ability against MCF-7 breast cancer cells. Compounds 5a and 5b seem to do the job pretty well. They were able to slow down the growth of these cancer cells, with 5a having an IC50 value of 24.6 ± 0.33 μg and 5b with 27.0 ± 0.28 μg. These results are promising because they suggest these compounds might be good at stopping cancer from spreading. In fact, they seem to work as well as, or even better than, some existing cancer drugs like Anastrozole, Lenvatinib, Vemurafenib, and Osimertinib. We also looked into how these compounds interact with a specific receptor called CDK4, which is important in cancer cells. It turns out that compounds 5a and 5b truly latch onto this receptor, which is good because it means they might specifically target cancer cells without harming healthy ones. We also checked if these compounds would cause any harm in the body. Fortunately, it seems that compounds 5a and 5b are highly safe, with no carcinogenic or hepatotoxic effects observed. They seem to get absorbed into the body well and can even pass through the blood–brain barrier without causing trouble, as suggested by the BOILED-Egg model study. These findings suggest that compounds 5a and 5b could be promising new treatments for breast cancer for being safer and more effective than some current treatments.

CRediT authorship contribution statement

Zainab H. Mahdi: Writing – original draft, Methodology. **Tahseen A. Alsalim:** Writing – review & editing, Supervision, Methodology, Data curation, Conceptualization. **Heider A. Abdulhussein:** Writing – review & editing, Visualization, Validation, Project administration, Data curation. **Ahmed A. Majed:** Writing – review & editing, Resources, Investigation, Formal analysis, Data curation, Conceptualization. **Sabah Abbas:** Writing – review & editing, Visualization, Validation, Project administration, Investigation, Data curation.

Declaration of competing interest

The authors declare that they have no known competing financial interests or personal relationships that could have appeared to influence the work reported in this paper.

Appendix A. Supplementary data

Supplementary data to this article can be found online at https://doi.org/10.1016/j.rechem.2024.101762.

References

[1] H. Weedon-Fekjær, B.H. Lindqvist, L.J. Vatten, O.O. Aalen, S. Tretli, Breast cancer tumor growth estimated through mammography screening data, Breast Cancer Res. 10 (2008) 1–13.
[2] A.N. Giaquinto, K.D. Miller, K.Y. Tossas, R.A. Winn, A. Jemal, R.L. Siegel, Cancer statistics for African American/black people 2022, CA Cancer J. Clin. 72 (3) (2022) 202–229.
[3] Miller KD, Ortiz AP, Pinheiro PS, Bandi P, Minihan A, Fuchs HE, et al. Cancer statistics for the US Hispanic/Latino population, 2021. CA: a cancer journal for clinicians. 2021;71(6):466-87.
[4] Giaquinto AN, Sung H, Miller KD, Kramer JL, Newman LA, Minihan A, et al. Breast cancer statistics, 2022. CA: a cancer journal for clinicians. 2022;72(6):524-41.
[5] R.L. Siegel, K.D. Miller, H.E. Fuchs, A. Jemal, Cancer statistics, 2021, Ca Cancer J Clin. 71 (1) (2021) 7–33.
[6] L.A. Huppert, O. Gumusay, D. Idossa, H.S. Rugo, Systemic therapy for hormone receptor-positive/human epidermal growth factor receptor 2-negative early stage and metastatic breast cancer, A Cancer Journal for Clinicians, CA, 2023.
[7] E. Clancy, ACS Report Shows Prostate Cancer on the Rise, Cervical Cancer on the Decline, Renal & Urology News. (2023) NA -NA.
[8] S. Senapati, A.K. Mahanta, S. Kumar, P. Maiti, Controlled drug delivery vehicles for cancer treatment and their performance, Signal Transduct. Target. Ther. 3 (1) (2018) 7.
[9] V. Mistiaen, Time and the great healer, The Guardian. (2002) 2.
[10] P. Martins, J. Jesus, S. Santos, L.R. Raposo, C. Roma-Rodrigues, P.V. Baptista, et al., Heterocyclic anticancer compounds: recent advances and the paradigm shift towards the use of nanomedicine's tool box, Molecules 20 (9) (2015) 16852–16891.
[11] S. Kakkar, S. Kumar, B. Narasimhan, S.M. Lim, K. Ramasamy, V. Mani, et al., Design, synthesis and biological potential of heterocyclic benzoxazole scaffolds as promising antimicrobial and anticancer agents, Chem. Cent. J. 12 (2018) 1 -.
[12] H. Sachdeva, J. Mathur, A. Guleria, Indole Derivatives As Potential Anticancer Agents: A Review, J. Chil. Chem. Soc., Concepción, Sept. 65 (3) (2020) 4900–4907.
[13] J. Zhao, J. Carbone, G. Farruggia, A. Janecka, L. Gentilucci, N. Calonghi, Synthesis and Antiproliferative Activity against Cancer Cells of Indole-Aryl-Amide Derivatives, Molecules 28 (1) (2022) 265.
[14] A.A. Singh, M.P. Patil, M.-J. Kang, I. Niyonizigiye, G.-D. Kim, Biomedical application of indole-3-carbinol: A mini-review, Phytochem. Lett. 41 (2021) 49–54.
[15] J.R. Weng, C.H. Tsai, S.K. Kulp, C.S. Chen, Indole-3-carbinol as a chemopreventive and anti-cancer agent, Cancer Lett. 262 (2) (2008 Apr 18) 153–163, https://doi.org/10.1016/j.canlet.2008.01.033.
[16] A. Kumari, R.K. Singh, Medicinal chemistry of indole derivatives: current to future therapeutic prospectives, Bioorg Chem. 89 (2019) 103021.
[17] P.V. Thanikachalam, R.K. Maurya, V. Garg, V. Monga, An insight into the medicinal perspective of synthetic analogs of indole: A review, Eur. J. Med. Chem. 180 (2019) 562–612.
[18] R. McDanell, A. McLean, A. Hanley, R. Heaney, G. Fenwick, Chemical and biological properties of indole glucosinolates (glucobrassicins): a review, Food Chem. Toxicol. 26 (1) (1988) 59–70.

[19] Ahmad A, A Sakr W, Wahidur Rahman K. Anticancer properties of indole compounds: mechanism of apoptosis induction and role in chemotherapy. Current drug targets. 2010;11(6):652-66.
[20] S. Stolc, Indole derivatives as neuroprotectants, Life Sci. 65 (18–19) (1999) 1943–1950.
[21] A. Agarwal, K. Srivastava, S.K. Puri, P.M.S. Chauhan, Synthesis of substituted indole derivatives as a new class of antimalarial agents, Bioorg Med Chem Lett 15 (12) (2005) 3133–3136.
[22] M.T. Macdonough, T.E. Strecker, E. Hamel, J.J. Hall, D.J. Chaplin, M.L. Trawick, K. G. Pinney, Synthesis and biological evaluation of indole-based, anti-cancer agents inspired by the vascular disrupting agent 2-(3'-hydroxy-4'-methoxyphenyl)-3-(3",4",5''-trimethoxybenzoyl)-6- methoxyindole (OXi8006), Bioorg Med Chem 21 (21) (2013) 6831–6843.
[23] Y. Yamamoto, M. Kurazono, Bioorg. Med. Chem. Lett. 17 (6) (2007) 1626–1628.
[24] S. Zhang, X. Wang, W. Yin, Z. Liu, M. Zhou, D. Xiao, et al., Bioorg. Med. Chem. Lett. 26 (19) (2016) 4799–4803.
[25] J. Wang, S. Lu, R. Sheng, J. Fan, W. Wu, R. Guo, Mini Rev. Med. Chem. 20 (17) (2020) 1791–1818.
[26] M. Emadi, F. Mosavizadeh-Marvest, A. Asadipour, Y. Pourshojaei, S. Hosseini, S. Mojtabavi, et al., BMC Chemistry. 17 (1) (2023) 1–14.
[27] Z. Bakherad, M. Safavi, A. Fassihi, H. Sadeghi-Aliabadi, M. Bakherad, H. Rastegar, et al., Res. Chem. Intermed. 45 (2019) 2827–2854.
[28] D. Veeranna, L. Ramdas, G. Ravi, S. Bujji, V. Thumma, J. Ramchander, ChemistrySelect 7 (29) (2022) e202201758.
[29] A. Dandia, S. Gupta, M. Quraishi, Journal of Materials and Environmental, Science 3 (5) (2012) 993–1000.
[30] D. Gupta, D. Jain, J. Adv. Pharm. Technol. Res. 6 (3) (2015) 141.
[31] M.K. Mohammed, Z. Al-Shuhaib, A.A. Al-Shawi, Mediterranean, J. Chem. 9 (4) (2019) 305–310.
[32] N.M. Nasir, T.A. Alsalim, A.A. El-Arabey, M. Abdalla, J. Biomol. Struct. Dyn. 41 (9) (2023) 3976–3992.
[33] S. Senapati, A.K. Mahanta, S. Kumar, et al., Sig Transduct Target Ther 3 (2018) 7, https://doi.org/10.1038/s41392-017-0004-3.
[34] P. Martins, J. Jesus, S. Santos, L.R. Raposo, C. Roma-Rodrigues, P.V. Baptista, A. R. Fernandes, Molecules 20 (2015) 16852–16891, https://doi.org/10.3390/molecules200916852.
[35] S. Kakkar, S. Kumar, B. Narasimhan, et al., Chem. Cent. J. 12 (2018) 96, https://doi.org/10.1186/s13065-018-0464-8.
[36] U. Aman, Buzdar, Expert Rev Anticancer Ther. 6 (2006 Jun) 839–848, https://doi.org/10.1586/14737140.6.6.839.
[37] S. Mayor, Lancet Oncol. 16 (3) (2015 Mar) e110.
[38] K.Y. Tsai, S. Nowroozi, K.B. Kim, Drug safety evaluation of vemurafenib in the treatment of melanoma, Expert Opin Drug Saf 12 (2013) 767–775.
[39] J.M. Sun, S.H. Lee, J.S. Ahn, K. Park, M.J. Ahn, Expert Opin Pharmacother 18 (2017) 225–231.
[40] A.N. Giaquinto, H. Sung, K.D. Miller, J.L. Kramer, L.A. Newman, A. Minihan, A. Jemal, R.L. Siegel, Breast Cancer Statistics, 2022, CA. *Cancer J. Clin.* 72 (2022) 524–541, https://doi.org/10.3322/caac.21754.
[41] S.L. Anwar, W.S. Avanti, A.C. Nugroho, L. Choridah, E.K. Dwianingsih, W. A. Harahap, et al., World J. Surg. Oncol. 18 (2020) 1–16.
[42] T. Liu, S. Song, X. Wang, J. Hao, Eur. J. Med. Chem. 210 (2021) 112954.
[43] B. Aruchamy, M.G. Kuruburu, V.R. Bovilla, S.V. Madhunapantula, C. Drago, S. Benny, et al., ACS Omega 8 (43) (2023) 40287–40298.
[44] H.A. El-Sherief, G.-E.-D.-A. Abuo-Rahma, M.E. Shoman, E.A. Beshr, R.M. Abdel-baky, Med. Chem. Res. 26 (2017) 3077–3090.
[45] A.K. Slavova-Kazakova, S.E. Angelova, T.L. Veprintsev, P. Denev, D. Fabbri, M. A. Dettori, et al., Beilstein J. Org. Chem. 11 (1) (2015) 1398–1411.
[46] C.A. Lipinski, Drug Discov. Today Technol. 1 (4) (2004) 337–341.
[47] C. Shivanika, D. Kumar, V. Ragunathan, P. Tiwari, A. Sumitha, J. Biomol. Struct. Dyn. (2020) 1.
[48] Shivanika C, DeepakKumar S., Venkataraghavan Ragunathan, Pawan Tiwari, Sumitha A. & Brindha Devi P, Journal of Biomolecular Structure and Dynamics, 40, (2022) , 585 611, DOI: 10.1080/07391102. 2020. 1815584.
[49] M. Abdalla, R.K. Mohapatra, A.K. Sarangi, P.K. Mohapatra, W.A. Eltayb, M. Alam, et al., J. Saudi Chem. Soc. 25 (12) (2021) 101367.
[50] R.K. Mohapatra, L. Perekhoda, M. Azam, M. Suleiman, A.K. Sarangi, A. Semenets, et al., Journal of King Saud University-Science. 33 (2) (2021) 101315.
[51] Ş. Adem, V. Eyupoglu, I. Sarfraz, A. Rasul, A.F. Zahoor, M. Ali, et al., Phytomedicine 85 (2021) 153310.
[52] D. De Vita, F. Pandolfi, L. Ornano, M. Feroci, I. Chiarotto, I. Sileno, et al., New N, Journal of Enzyme Inhibition and Medicinal, Chemistry 31 (sup4) (2016) 106–113.
[53] Czechtizky W, Hamley P., Wiley Online Library; 2015.
[54] U. Singh, R.P. Gangwal, G.V. Dhoke, R. Prajapati, M. Damre, A.T. Sangamwar, Arab. J. Chem. 10 (2017) S617–S626.
[55] P. Keglevich, L. Hazai, G. Kalaus, C. Szántay, Molecules 17 (5) (2012 May) 5893–5914.
[56] B. Biersack, R. Schobert, Curr. Drug Targets 13 (2012) 1705–1719.
[57] S. Salerno, E. Barresi, E. Baglini, V. Poggetti, F. Da Settimo, S. Taliani, Molecules 28 (6) (2023 Mar) 2587.
[58] H. Masuda, D. Zhang, C. Bartholomeusz, H. Doihara, G.N. Hortobagyi, N.T. Ueno, Breast Cancer Res. Treat. 136 (2012) 331–345.
[59] S. Mokhtari, M. Mosaddegh, M. Hamzeloo Moghadam, Z. Soleymani, S. Ghafari, F. Kobarfard, Iran. J. Pharm. Res. IJPR 11 (2012) 411–421.
[60] V.T. Angelova, T. Tatarova, R. Mihaylova, N. Vassilev, B. Petrov, Z. Zhivkova, I. Doytchinova, Molecules 28 (5) (2023) 2058.
[61] C. Hong, G.L. Firestone, L.F. Bjeldanes, Biochem. Pharmacol. 63 (2002) 1085–1097, https://doi.org/10.1016/S0006-2952(02)00856-0.
[62] S.S. Mirfazli, F. Kobarfard, L. Firoozpour, A. Asadipour, M. Esfahanizadeh, K. Tabib, et al., DARU Journal of Pharmaceutical Sciences. 22 (2014) 1–10.